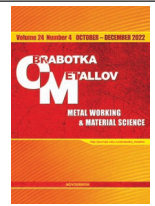




# Obrabotka metallov - Metal Working and Material Science

Journal homepage: [http://journals.nstu.ru/obrabotka\\_metallov](http://journals.nstu.ru/obrabotka_metallov)



## Development of plasma cutting technique for C1220 copper, AA2024 aluminum alloy, and Ti-1,5Al-1,0Mn titanium alloy using a plasma torch with reverse polarity

Valery Rubtsov <sup>a, \*</sup>, Alexander Panfilov <sup>b</sup>, Knyazhev Evgeny <sup>c</sup>, Alexandra Nikolaeva <sup>d</sup>, Andrey Cheremnov <sup>e</sup>,  
 Anastasia Gusarova <sup>f</sup>, Vladimir Beloborodov <sup>g</sup>, Chumaevskii Andrey <sup>h</sup>, Ivanov Alexey <sup>i</sup>

Institute of Strength Physics and Materials Science of Siberian Branch of Russian Academy of Sciences, 2/4, pr. Akademicheskii, Tomsk, 634055, Russian Federation

<sup>a</sup> <https://orcid.org/0000-0003-0348-1869>, [rvy@ispms.tsc.ru](mailto:rvy@ispms.tsc.ru), <sup>b</sup> <https://orcid.org/0000-0001-8648-0743>, [alexpl@ispms.ru](mailto:alexpl@ispms.ru),  
<sup>c</sup> <https://orcid.org/0000-0002-1984-9720>, [clothoid@ispms.tsc.ru](mailto:clothoid@ispms.tsc.ru), <sup>d</sup> <https://orcid.org/0000-0001-8708-8540>, [nikolaeva@ispms.tsc.ru](mailto:nikolaeva@ispms.tsc.ru),  
<sup>e</sup> <https://orcid.org/0000-0003-2225-8232>, [amc@ispms.tsc.ru](mailto:amc@ispms.tsc.ru), <sup>f</sup> <https://orcid.org/0000-0002-4208-7584>, [gusarova@ispms.ru](mailto:gusarova@ispms.ru),  
<sup>g</sup> <https://orcid.org/0000-0003-4609-1617>, [vabel@ispms.tsc.ru](mailto:vabel@ispms.tsc.ru), <sup>h</sup> <https://orcid.org/0000-0002-1983-4385>, [tch7av@gmail.com](mailto:tch7av@gmail.com),  
<sup>i</sup> <https://orcid.org/0000-0001-8959-8499>, [ivan@ispms.tsc.ru](mailto:ivan@ispms.tsc.ru)

### ARTICLE INFO

#### Article history:

Received: 21 September 2022  
 Revised: 04 October 2022  
 Accepted: 03 November 2022  
 Available online: 15 December 2022

#### Keywords:

Plasma cutting  
 Titanium alloy Ti-1,5Al-1,0Mn  
 Macrostructure  
 Copper C1220  
 Aluminum alloy AA2024  
 Heat-affected zone  
 Changes in the mechanical properties of the material  
 Disturbance of the macrogeometry of the cut

#### Funding

The results were obtained in the framework of the Integrated Project "Establishment of production of high-tech equipment for adaptive high-precision plasma heavy cutting of non-ferrous metals for the metallurgical, aerospace and transport industries of the Russian Federation" (Agreement No. 075-11-2022-012 dated April 06, 2022) implemented by the ISPMS SB RAS at the financial support of the Ministry of Education and Science of the Russian Federation as part of Decree of the Government of the Russian Federation No. 218 dated April 09, 2010.

#### Acknowledgements

Research were partially conducted at core facility "Structure, mechanical and physical properties of materials".

### ABSTRACT

**Introduction.** An important area of research in the field of plasma metal cutting is obtaining a metal cut face characterized by minimal roughness and geometric deviations. It is also important to minimize changes in the structure of the metal under the cutting surface caused by the temperature effects of the plasma jet, including the formation of dross. The solution to the problem of obtaining a quality cut is to optimize the parameters of the cutting process. The plasma arc current and voltage, cutting height and cutting speed are considered to be the main parameters that determine cut quality. However, insufficient attention has been paid to the processes of plasma metal cutting of thicknesses above 20 mm due to the limitations associated with the operation conditions of plasma torches with direct polarity currents. Accordingly, for cutting large thicknesses, the use of a plasma torch operating on currents of reverse polarity seems promising. **The aim of this work** is to develop the technique of plasma cutting of copper, titanium and aluminum alloy sheets up to 40 mm thick using a plasma torch operating on currents of reverse polarity. **Results and discussion.** Investigations show that for cutting aluminum alloy (*Al* 90.9–94.7 %; *Cu* 3.8–4.9 %; *Mg* 1.2–1.8 %; *Mn* 0.3–0.9 %) and titanium alloy (*Ti* 94.33–97.5 %; *Al* 1.5–2.5 %; *Mn* 0.7–2.0 %) it is possible to regulate the cutting speed in a wide range, while for rolled copper (*Cu* ≥99.96 %) and aluminum alloy with thickness of 40 mm the range of cutting speed regulation is rather narrow. While for aluminum alloy due to excessive precipitation of alloying elements from the solid solution in the heat-affected zone decrease of microhardness is observed, for titanium alloy the microhardness growth due to material hardening is characteristic. Changing the cutting mode parameters allows receiving more homogeneous macrogeometry of a cutting surface, smaller depth of a zone of melting of a material and a heat-affected zone and smaller changes of mechanical properties of a material in a zone of a cut. For the titanium alloy, almost all of the cutting modes used are close to optimum. For alloy aluminum and copper the modes providing the best cutting quality in the considered range of parameters are determined. According to the results of the work it can be concluded that plasma cutting on reverse polarity currents is effective for cutting rolled products of large thicknesses, but the technique requires further development in order to improve the quality of the resulting cut.

**For citation:** Rubtsov V.E., Panfilov A.O., Knyazhev E.O., Nikolaeva A.V., Cheremnov A.M., Gusarova A.V., Beloborodov V.A., Chumaevskii A.V., Ivanov A.N. Development of plasma cutting technique for C1220 copper, AA2024 aluminum alloy, and Ti-1,5Al-1,0Mn titanium alloy using a plasma torch with reverse polarity. *Obrabotka metallov (tehnologiya, oborudovanie, instrumenty) = Metal Working and Material Science*, 2022, vol. 24, no. 4, pp. 33–52. DOI: 10.17212/1994-6309-2022-24.4-33-52.

### \*Corresponding author

Rubtsov Valery Evgenievich, Leading researcher  
 Institute of Strength Physics and Materials Science of Siberian Branch  
 of Russian Academy of Sciences,  
 2/4, pr. Akademicheskii,  
 634055, Tomsk, Russian Federation  
 Tel.: 8 (382) 228–68–63, e-mail: [rvy@ispms.ru](mailto:rvy@ispms.ru)

## Introduction

Plasma cutting of metals is an integral part of production processes in various engineering industries. Although the cut quality of plasma cutting may be inferior to, for example, waterjet or laser cutting [1], but its advantage is the optimal combination of technological capabilities, simplicity of equipment setup and productivity, also when cutting metal with a thickness of more than 100 mm [2].

To date, a number of research in the field of plasma metal cutting are being conducted. An important area of research is to obtain a metal cut surface characterized by minimal roughness and geometric variations [3–6]. Also, minimizing changes in metal structure under cut surface caused by temperature effects of plasma jet, including dross formation, is important as well [7–10]. These trends form the main task of research: obtaining a quality cut, as geometric and structural changes in material are usually removed by further processing, the minimization of allowances for which determines the effectiveness of the plasma cutting process.

To solve this problem, researchers have proposed a number of methods related both to changes in equipment realization of a cutting process, and to optimization of its parameters [11–14]. Methods of cutting parameters optimization involve the application of various methods of mathematical modeling, establishing a relationship between geometric and structural parameters of a material in the area of cutting and a range of parameters of a cutting process. Among the main parameters that determine the quality of the cut, plasma arc current and voltage, cutting height, and cutting speed are considered [15–17].

However, all studies are carried out, mainly, with consideration of cut metals with a thickness of up to 20 mm and insufficient attention is paid to cutting of metals with greater thicknesses. According to the authors, this is due, primarily, to the limitations associated with the operating conditions of cutting plasmatrons. The most widely used plasmatrons with thermochemical cathodes and operating at direct current polarity have limitations in terms of capacity and the number of switchings, which is associated with the temperature mode of operation, as well as the wear of cathode inserts made of relatively expensive and rare metals [18–20]. For cutting metals of large thicknesses the method of cutting with currents of reversed polarity seems promising, in which the supporting spot of the cutting arc is significantly deepened in the cutting cavity, and the distribution of heat input to the cutting front edge along the height of it is more uniform. Due to this, it becomes possible to cut metals of large thicknesses, a better quality of cut along the bevel of edges, and a smaller width of the cutting cavity [21–22].

Considering the above, the main purpose of the present work is to develop methods of plasma cutting of copper, titanium and aluminum alloy sheets with thickness up to 40 mm using plasmatron, working with currents of reverse polarity. An additional task is to determine the influence of sheet thickness and non-standard arrangement of the plates on the structure of the cutting edge.

## Research methodology

Experimental research was carried out on the production site in LLC “ITS-Siberia”. Cutting was carried out on a plasmatron with reverse polarity. The exterior of the plasma cutter is shown in Fig. 1. The machine consists of a work table for placing workpieces, a plasmatron, a moving carriage and guides to move a plasmatron. It also includes a gas preparation unit and a power unit. Nitrogen is used as protective gas.

Rolled sheets of copper *C1220* ( $Cu \geq 99.96\%$ ) with thickness of 40 mm, aluminum alloy *AA2024* ( $Al\ 90.9\text{--}94.7\%$ ;  $Cu\ 3.8\text{--}4.9\%$ ;  $Mg\ 1.2\text{--}1.8\%$ ;  $Mn\ 0.3\text{--}0.9\%$ ) with thickness of 12 and 40 mm, and titanium alloy *Ti-1.5Al-1.0Mn* ( $Ti\ 94.33\text{--}97.5\%$ ;  $Al\ 1.5\text{--}2.5\%$ ;  $Mn\ 0.7\text{--}2.0\%$ ) with thickness of 5 and 10 mm were used as experimental material. In order to form specimens from a 10 mm thick titanium alloy, two 5 mm thick sheets stacked together were used. This was done to further reveal the specifics of cutting packages of sheets, which change significantly in the presence of the interface between the sheets being cut. The cutting process parameters used in the research are given in Table 1.

Plasma cutting process parameters were determined empirically based on typical parameters used for cutting metals and alloys on conventional equipment. Length of a cutting cut was varied from 100 to 300 mm. Parameters were adjusted until a relatively uniform cut was achieved, which was determined



Fig. 1. Plasma cutter:

*a* – plasma cutter appearance; *b* – an image of the cutting process; *c* – plasmatron appearance; 1 – work table; 2 – plasmatron; 3 – carriage; 4 – linear guides for transverse movement; 5 – linear guides for longitudinal movement

Table 1

Plasma cutting modes

Alloy	$S$ , mm	Mode No.	Delay of pierce, s	Height of pierce, mm	Cutting height, mm	$I$ , A	$U$ , V	$V$ , mm/min
Ti-1.5Al-1.0Mn	5	1	0.4	6.07	2.54	130	154	2,400
Ti-1.5Al-1.0Mn	5	2	0.4	6.07	2.54	130	154	2,000
Ti-1.5Al-1.0Mn	5	3	0.4	6.07	2.54	130	154	1,600
Ti-1.5Al-1.0Mn	10	1	0.5	6.07	2.54	130	171	1,600
Ti-1.5Al-1.0Mn	10	2	0.5	6.07	2.54	130	171	1,200
Ti-1.5Al-1.0Mn	10	3	0.5	6.07	2.54	130	171	1,400
AA2024	12	1	0.4	–	3.81	300	170	4,542
AA2024	12	2	0.4	–	3.81	300	170	3,000
AA2024	12	3	0.4	–	3.81	300	170	2,000
AA2024	12	4	0.4	–	3.81	300	170	6,000
AA2024	12	5	0.4	–	3.81	300	170	8,000
AA2024	40	1	0.6	–	6.35	300	205	559
AA2024	40	2	0.4	–	6.35	300	205	559
AA2024	40	3	0.6	–	6.35	300	205	450
AA2024	40	4	0.6	–	6.35	300	205	400
AA2024	40	5	0.6	–	6.35	300	205	300
AA2024	40	6	0.6	–	4.0	300	205	300
AA2024	40	7	0.4	–	4.0	300	205	300
AA2024	40	8	0.6	–	4.0	300	205	650
AA2024	40	9	0.6	–	4.0	300	205	750
AA2024	40	10	0.6	–	4.0	300	205	800
CI220	40	1	0.5	6.35	6.35	300	205	450
CI220	40	2	2.0	6.35	4.35	300	205	450
CI220	40	3	2.0	6.35	4.35	300	205	300
CI220	40	4	4.0	6.35	4.35	300	205	250
CI220	40	5	6.0	6.35	4.35	300	205	150
CI220	40	6	6.0	4.0	4.35	300	205	150
CI220	40	7	6.0	4.0	4.35	300	205	100

using visual and dimensional control. Methodologically, the work was structured so that during the tests an optimal cutting speed, required for the fastest obtaining of a high-quality cutting with the smallest distortions of macrogeometry, the zone of thermal influence and the most uniform cutting surface were determined. For this purpose, different parameters of current and cutting speed were initially used. Then, if the cutting quality was acceptable, the cutting speed was increased. If the cutting quality was unsatisfactory, the cutting speed was reduced. Additionally, the parameters of piercing time and height, cutting height, etc. were determined.

After carrying out the experiments on plasma cutting, analysis of specimens' cut surface by means of visual measuring control with taking a picture of a surface by camera *Pentax K-3* with focal distance of objective 100 mm was made. An optical microscope *Altami MET 1C* was used for metallographic examination of specimens. Microhardness was determined using a *Duramin 5* microhardness tester. Measurements of microhardness were carried out on metallographic thin sections starting from a distance of 10  $\mu\text{m}$  from the cutting surfaces. A depth, to which changes in microhardness were determined, was chosen from the size of a heat-affected zone. Cutting out samples for research was carried out by the method of electrical discharge on wire cut *EDM* machine *DK7750* transverse to a plane of the cut. In addition, using a confocal microscope *Olympus LEXT 4100* the cut surfaces were evaluated by determining the height of roughness above the cut surface. General conclusions about the quality of the cutting were formulated based on the evaluation of all the main factors and depended on the total depth of microroughness from the cut surface, macrogeometry disturbance and the heat-affected zone. Additionally, a location of these defects was taken into account; since the macrogeometric disturbances of the cut surface and the heat-affected zone are partially overlap.

## Results and discussion

During the process of plasma cutting of specimens of metals and alloys a specific relief with different structure for different alloys is formed on the cut surface. For example, the cut surface of titanium alloy for most samples is characterized by the presence of a regular relief that differs in the upper and lower parts (1, 2 in Fig. 2, *a*). Moreover, the appearance of the sample surface in the upper and lower parts of the cut differs clearly enough, which may be related to different features of blowing of molten metal by the gas jet from the cutting zone.

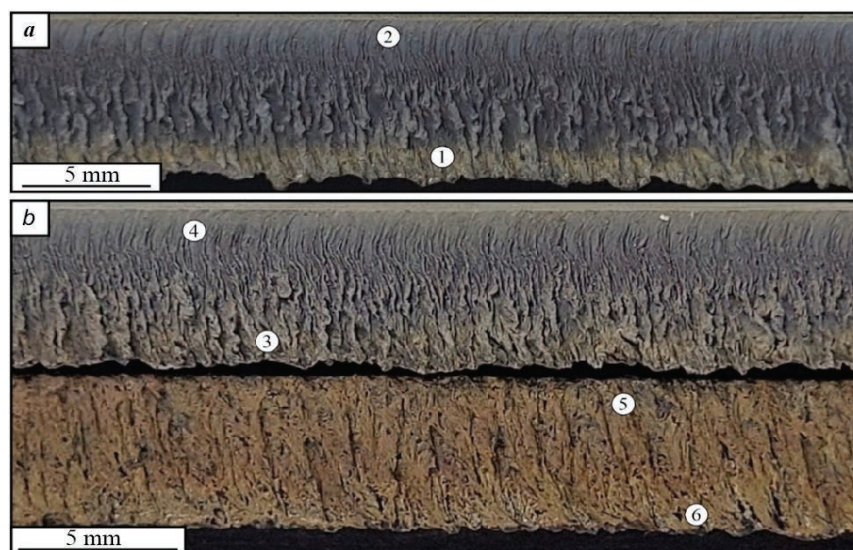


Fig. 2. Appearance of the cut face of the titanium alloy samples:

*a* – the plate is 5 mm thick; *b* – two plates are 5 mm thick; 1 – bottom of the cut face; 2 – top of the cut face; 3 – bottom of the cut face of upper plate; 4 – top of the cut face of upper plate; 5 – top of the cut face of lower plate; 6 – bottom of the cut face of lower plate

In the upper part of the specimen the height of roughness peaks above the cut surface is 70–75  $\mu\text{m}$  in average, while in the lower part it is more than 245–275  $\mu\text{m}$  depending on the cutting mode (the lowest values are characteristic for the mode with the cutting speed of 2,000 mm/min according to Table 1). These peaks are formed by flows of molten metal blown by the gas jet from the cutting zone, quickly solidifying when the plasmatron withdraws from the cutting point. As can be seen from the optical photographs and from the results of laser scanning microscopy, the peaks in the upper part of the cut, in addition to its smaller size, can be characterized by a smaller distance between it in comparison with the peaks in the lower part of the specimen. On the cut surface in both the upper and lower parts of the specimen, it is possible to see quite obvious features of oxidation (Fig. 2, *a*), despite the use of shielding gas in the cutting process. In the lower part of the cut, it is possible to distinguish an irregularity of the edge, which is formed during cutting as a result of blowing of metal from the area of the cut, and its crystallization with formation of a small amount of flowed metal.

During plasma cutting of 10 mm thick specimens of titanium alloy *Ti-1.5Al-1.0Mn*, due to the increased material thickness and superimposed sheets, displacement of molten metal from the cutting zone was difficult. For this reason, the differences in the features of the structure of the upper and lower parts of the cut become even more significant. Figure 2, *b* shows images of the cut surface of the upper and lower plate after cutting under mode No. 1 (Table 1).

The surface of the top plate after cutting is quite close to that previously observed on specimens with a thickness of 5 mm. In the upper part of the upper plate, the height of irregularities above the cut surface is not more than 110–150  $\mu\text{m}$ , while at the bottom of the plate it can reach 205–215  $\mu\text{m}$  and more. Significantly larger irregularities and heterogeneity of the surface structure are characteristic for the lower plate. In the upper part of the lower plate, the size of irregularities is up to 200–305  $\mu\text{m}$ , and in the lower part it is up to 330–680  $\mu\text{m}$ . The smallest sizes of peaks and valleys are characteristic for the specimens obtained by the mode No. 1. Periodicity of the formed peaks on the cut surface changes from the upper to the lower part of the plates. The smallest distance between the peaks can be observed in the upper part of the upper plate. Further towards the lower part of the cut there is an increase in the distance between irregularities, which reaches a maximum in the lower plate. In spite of the largest size of irregularities on the cut surface in the lower plate, the cut with the most homogeneous distribution of peaks and valleys is formed on it. In the lower plate, the cut is almost unchanged in height or along the length of the plate. The direction of the formed peaks on the cut surface of the lower plate also does not change, while in the upper plate it significantly changes from the top to the bottom. On the cutting surfaces of both the upper and lower plates, it is possible to identify marks of oxidation of the material (Fig. 2, *b*). Moreover, oxidation, according to the appearance of the surface, varying degrees occurs at the top and bottom plate. In the lower part of the plates, formation of small amount of flowed metal in both plates is detected, but in the lower plate the overlap is significantly smaller and the lower edge of the cut is more uniform along the length of the plate.

Parameters of plasma cutting modes of *AA2024* aluminum alloy with thickness of 12 mm were determined using the parameters given in Table 1. Low cutting speed (mode No. 3) of *AA2024* alloy specimens with thickness of 12 mm causes low quality of the cut surface (Fig. 3, *a*). In this case, there are drastic differences between the upper and lower cutting zones, with the presence of small and quasi-periodic relief elements in the upper part and large elements in the lower part. At higher cutting speeds (mode No. 4) a rather homogeneous cut surface is obtained (Fig. 3, *b*). The size of irregularities above the cut surface was 50–150  $\mu\text{m}$  in the upper part of the cut and 80–260  $\mu\text{m}$  in the lower part. The smallest irregularities are characteristic for the specimens obtained according to mode No. 4. No clearly visible oxides or any inclusions of other character were identified on the cut surfaces as well.

During plasma cutting of specimens of aluminum alloy *AA2024* with thickness of 40 mm a number of specific features were detected. In this case, the heating of the material of the cutting zone is of great importance, as a result of which at the beginning of the cut almost all samples have a deviation of the cutting axis location from the preset position (Fig. 4). There are a large number of relief elements on the cut surface, and its arrangement in the upper part is more ordered than in the lower one of the sample. In the lower part of the cutting zone, a small amount of metal is noted, which forms local areas of flowed metal, which

shows a better removal of the molten metal from the cut cavity. Significant heterogeneity of the cut surface, including macroscopic size, is characteristic for the specimens obtained according to non-optimal modes (mode No. 9, Fig. 4, *a*). The specimens obtained using more optimal modes are characterized by a more uniform structure of the cut surface (mode No. 7, Fig. 4, *b*). The size of peaks above the cutting surface is 200–470  $\mu\text{m}$  in the upper part and 230–600  $\mu\text{m}$  in the lower part.

During plasma cutting of *C1220* copper specimens, the formation of the largest amounts of flowed metal are observed in the lower part of the cutting (Fig. 5). This is due to the high thermal conductivity of copper and indicates that the molten metal, blown by the gas jet from the cut cavity, solidified at a fairly high rate. In many areas of the cut, the amounts of flowed metal are almost missing, but by adjusting the parameters of the cutting mode it was not possible to achieve its complete absence. The size of irregularities on the cut surface is 25–80  $\mu\text{m}$  at the top and 65–200  $\mu\text{m}$  at the bottom of the cut. The lowest values of irregularities heights are characteristic for the specimens obtained by the mode No. 5.

Studies of the structure of *Ti-1.5Al-1.0Mn* alloy samples with a thickness of 5 mm in cross-section to the cutting plane showed that in the specimens there is quite a significant distortion of the macrogeometry of the cut, especially in the upper part of the specimen (Fig. 6, *a, b*). Also the size of a heat-affected zone differs significantly (Fig. 6, *b, c*), having 415–520  $\mu\text{m}$  in the upper part of the cut and 800–1,820  $\mu\text{m}$  in the lower part. Smaller sizes are characteristic for the mode No. 2. At the bottom of the cutting zone amounts of flowed metal with dendritic structure are clearly distinguished (Fig. 6, *c*). This is caused by displacement of molten metal from the cut zone, its flowing down to the lower part of the cut and solidification as a flowed metal.

Studies of regularities of structure organization at higher magnification show that structural changes during cutting under different modes are typical for this type of alloys. In the bulk metal zone (Fig. 6, *d*) a typical structure with grains elongated in the direction of rolling is characteristic.



Fig. 3. Cut faces appearance of specimens of aluminum alloy with a thickness of 12 mm:  
*a* – specimen after cutting in non-optimal mode; *b* – specimen after cutting in optimal mode; 1 – bottom of the cut face; 2 – top of the cut face

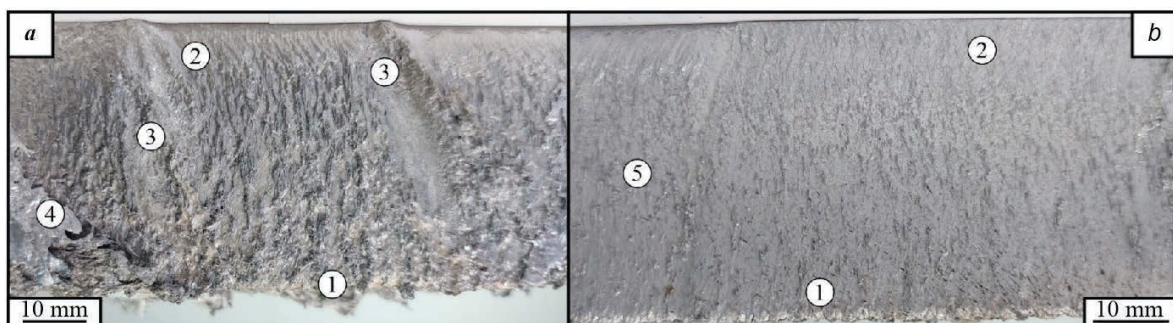


Fig. 4. Cut faces appearance of specimens of aluminum alloy with a thickness of 40 mm:  
*a* – specimen after cutting in non-optimal mode; *b* – specimen after cutting in optimal mode; 1 – bottom of the cut face; 2 – top of the cut face; 3 – macrodefects of the cut face; 4, 5 – defects in the initial part of the cut face

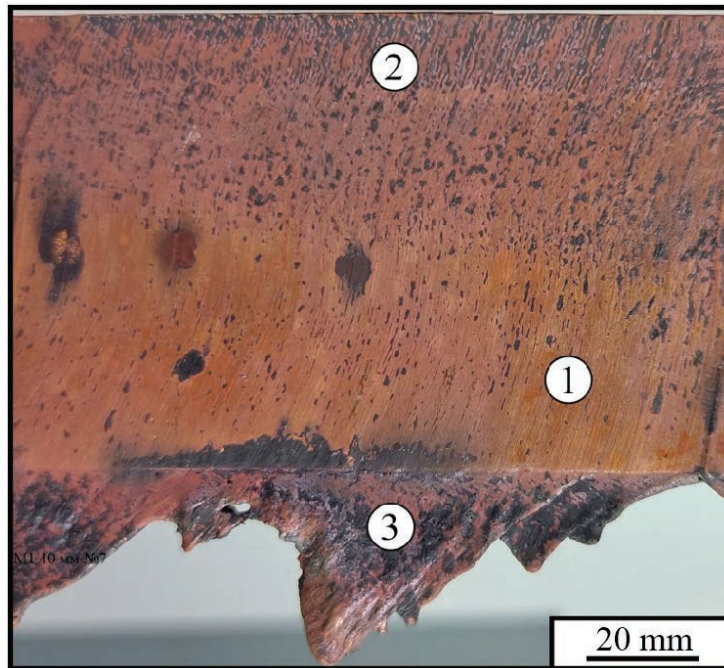


Fig. 5. Cut faces appearance of specimens of copper with a thickness of 40 mm:

1 – bottom of the cut face; 2 – top of the cut face; 3 – a flowed metal

In the heat-affected zone, a heating above the temperature of polymorphic transformation and subsequent hardening occurs with the formation of a needle-like structure, which is close for all three cutting modes (Fig. 6, *e*). The zone of metal melting which is mainly located in the area of flowed metal is represented by a dendritic structure (Fig. 6, *f*) formed with sufficiently rapid crystallization from the liquid state, which leads to formation of rather fine dendrites. The described changes in the cut zone structure inevitably lead to changes in the mechanical properties of the material, which can be unacceptable in various conditions. To investigate changes of mechanical properties of a cut surface further in the work, measurements of microhardness of a near-surface zone were carried out. The results of measurements of microhardness in specimens show, that in the heat-affected zone there is an increase in microhardness of the material (Fig. 6, *g, h*) both in the top, and in the bottom parts of the specimen. At distance of up to 2,000  $\mu\text{m}$  from the cut surface, the microhardness values are at a level close to the base metal. In general, all of the three selected modes are quite well suited for obtaining parts by plasma cutting. From the viewpoint of the smallest values of the allowance for the further processing, mode No. 2 can be considered more optimal, characterized by an average cutting speed and the smallest depth of the heat-affected zone (up to 880  $\mu\text{m}$ ). It should be noted that during cutting of titanium alloy a metal hardening occurs in the heat-affected zone with an increase in microhardness, which can reduce the machinability of the material during further edge milling.

The structure of the cutting zone of the titanium alloy *Ti-1.5Al-1.0Mn* specimens consisting of two plates with thickness of 5 mm, stacked in a package, is similar enough to that described earlier (Fig. 7, *a*). In the upper part of the upper plate a significant distortion of macrogeometry is observed, and the heat affected zone increases to the bottom of both plates (Fig. 7, *a-d*). At the same time, the lower plate is characterized by a rather uniform shape of the cut edge. In this case, only a small amount of remelted material is located on the cut surface of the upper plate, while the cut surface of the lower plate may have a rather thick layer with a dendritic structure (Fig. 7, *a, d, e*). The size of the heat-affected zone in the upper part of the upper plate is 550–700  $\mu\text{m}$ , in the bottom part – 1,150–1,300  $\mu\text{m}$ , in the upper part of the lower plate – 800–950  $\mu\text{m}$ , in its bottom part – 1,900–2,300  $\mu\text{m}$ . The smallest sizes of the heat-affected zone are characteristic for the cutting mode No. 1. The melted zone metal is fairly unevenly distributed over the cut surface. Between the molten metal and the base metal of the specimen, the formation of defects in the form of pores

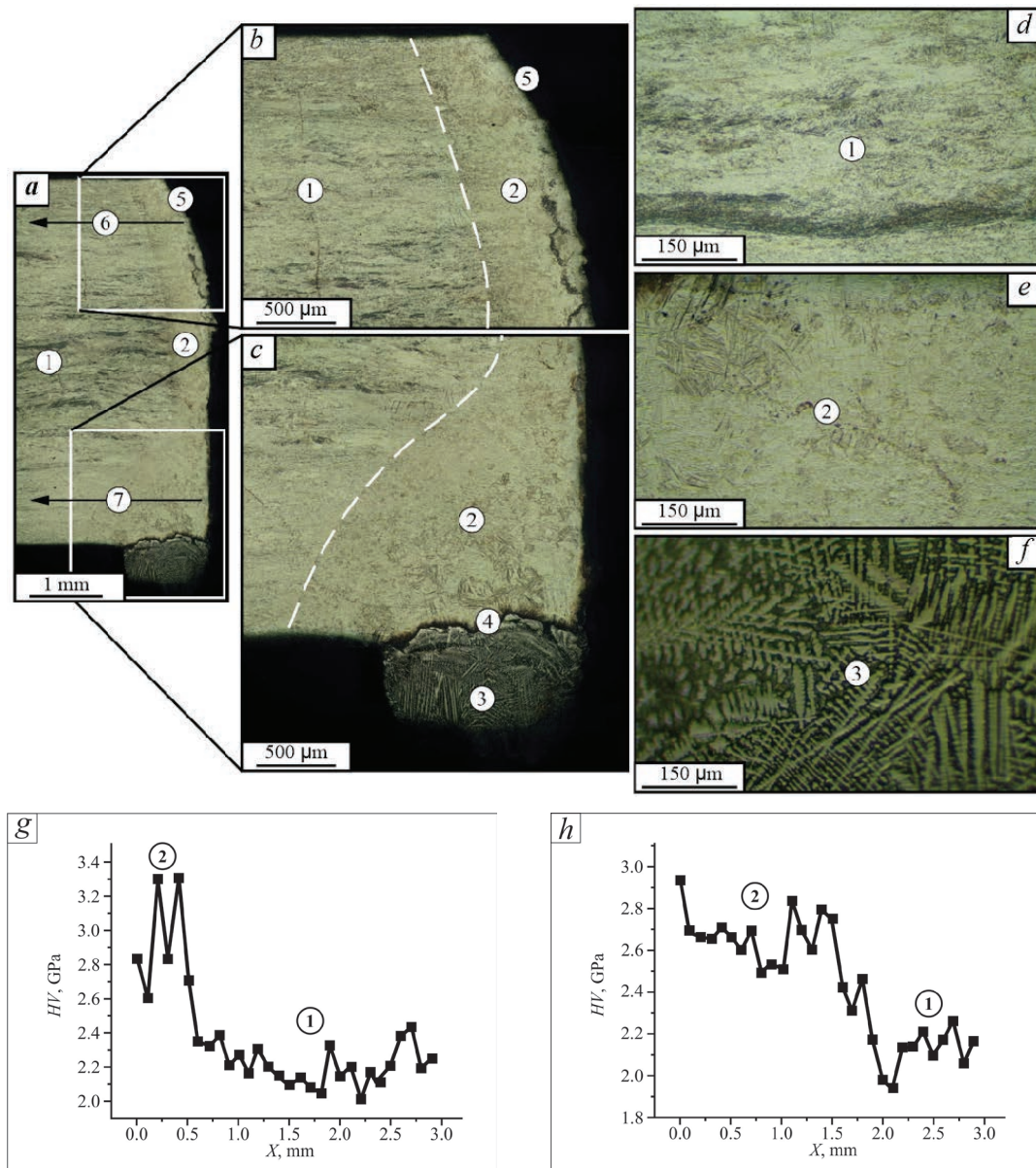


Fig. 6. Macro- and microstructure of typical specimen of titanium alloy with a thickness of 5 mm after plasma cutting:

*a* – macrostructure; *b, c* – enlarged images of the upper and lower parts of cut zone; *d, e, f* – microstructure of specific zones; *g, h* – microhardness variation; 1 – base metal; 2 – heat-affected zone; 3 – melting zone; 4 – zone boundary; 5 – macrogeometry failure; 6, 7 – areas of microhardness testing

or discontinuities occurs. These regions should be removed during further machining of the material. The organization of the structure within the typical structural zones of the specimens is similar to that observed when cutting specimens with a thickness of 5 mm. Microhardness measurements (Fig. 7, *e-i*) also show that in the boundary area there is a drastic increase in the microhardness of the material compared to the base metal. The research shows a fairly high degree of applicability of all three modes of plasma cutting of specimens with a total thickness of 10 mm, similarly to the cutting of specimens with a thickness of 5 mm. Mode No. 1 is the most optimal, since it is characterized by a shallower depth of the heat-affected zone.

Structural changes in the plasma cutting zone of AA2024 alloy specimens with a thickness of 12 mm differ from those previously described for titanium alloy (Fig. 8). All samples under study are characterized by the presence of a metal melting zone, a heat-affected zone, and a base metal with an unchanged structure. For the most of the specimens, it is possible to identify macrogeometric distortions and the flowed metal formation from the material remelted in the cutting cavity and accumulated in the lower part of the cut.

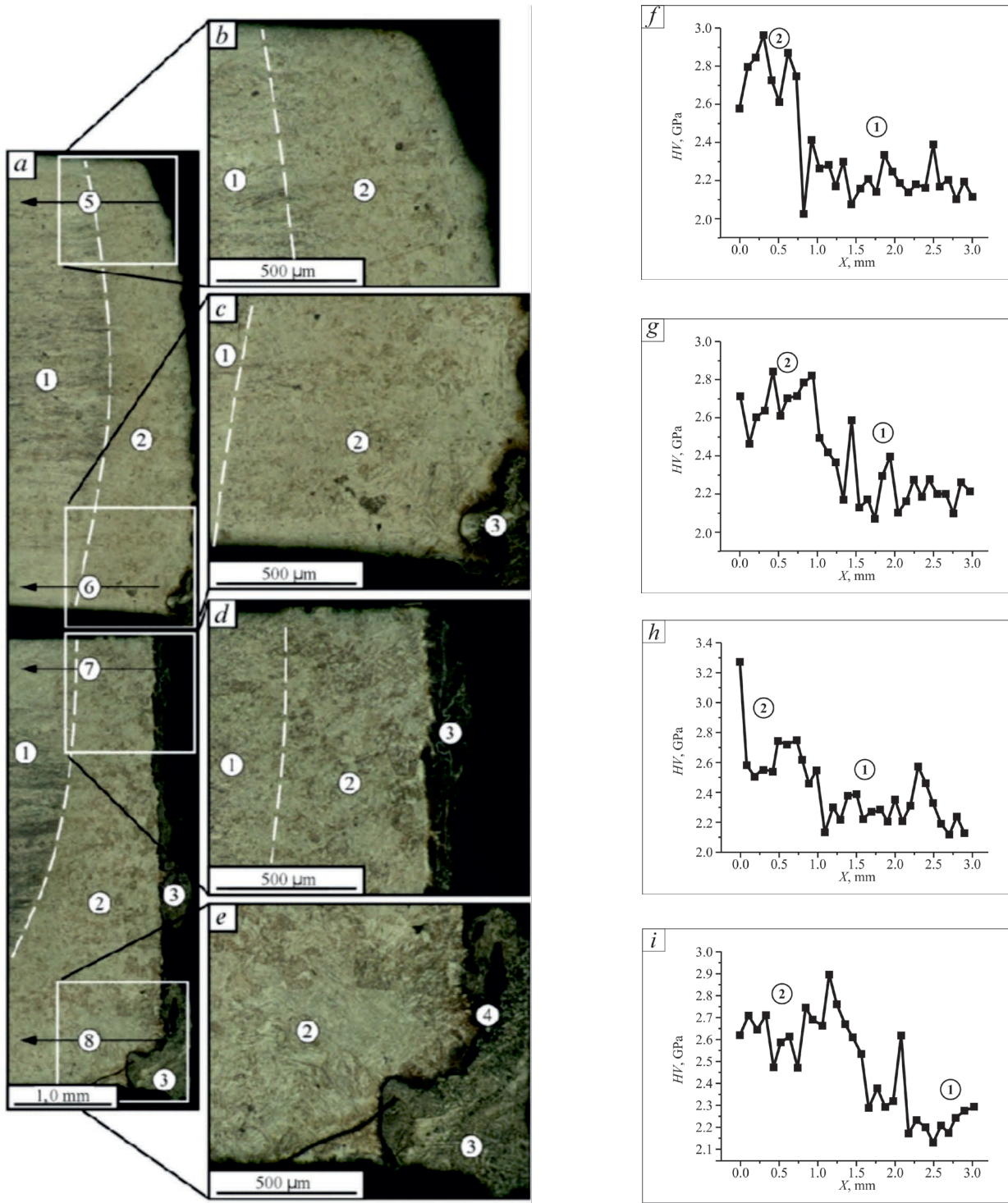


Fig. 7. Macro- and microstructure of typical package specimen of two sheets of titanium alloy with a thickness of 5 mm after plasma cutting:

*a* – macrostructure; *b–e* – microstructure of specific zones; *f–i* – microhardness variation; 1 – base metal; 2 – heat-affected zone; 3 – melting zone; 4 – zone boundary; 5–8 – areas of microhardness testing

The heat-affected zone in specimens is represented by an almost undeformed structure of the base metal with enhanced etchability relative to it (Fig. 8, *a–c*). The size of the heat-affected zone is about 100–200 μm in the upper part and 600–2,000 μm in the bottom part, with the lowest values for mode No. 2. All specimens are characterized by an identical structure in the initial state (Fig. 8, *d*). In the melting zone a typical structure with dendritic texture is formed when molten metal flows down the cut surface (Fig. 8, *g*). Due to the high rate of crystallization of the metal on the cut surface, formation of a fine dendritic texture and defects in the form of cracks occurs (Fig. 8, *e*).

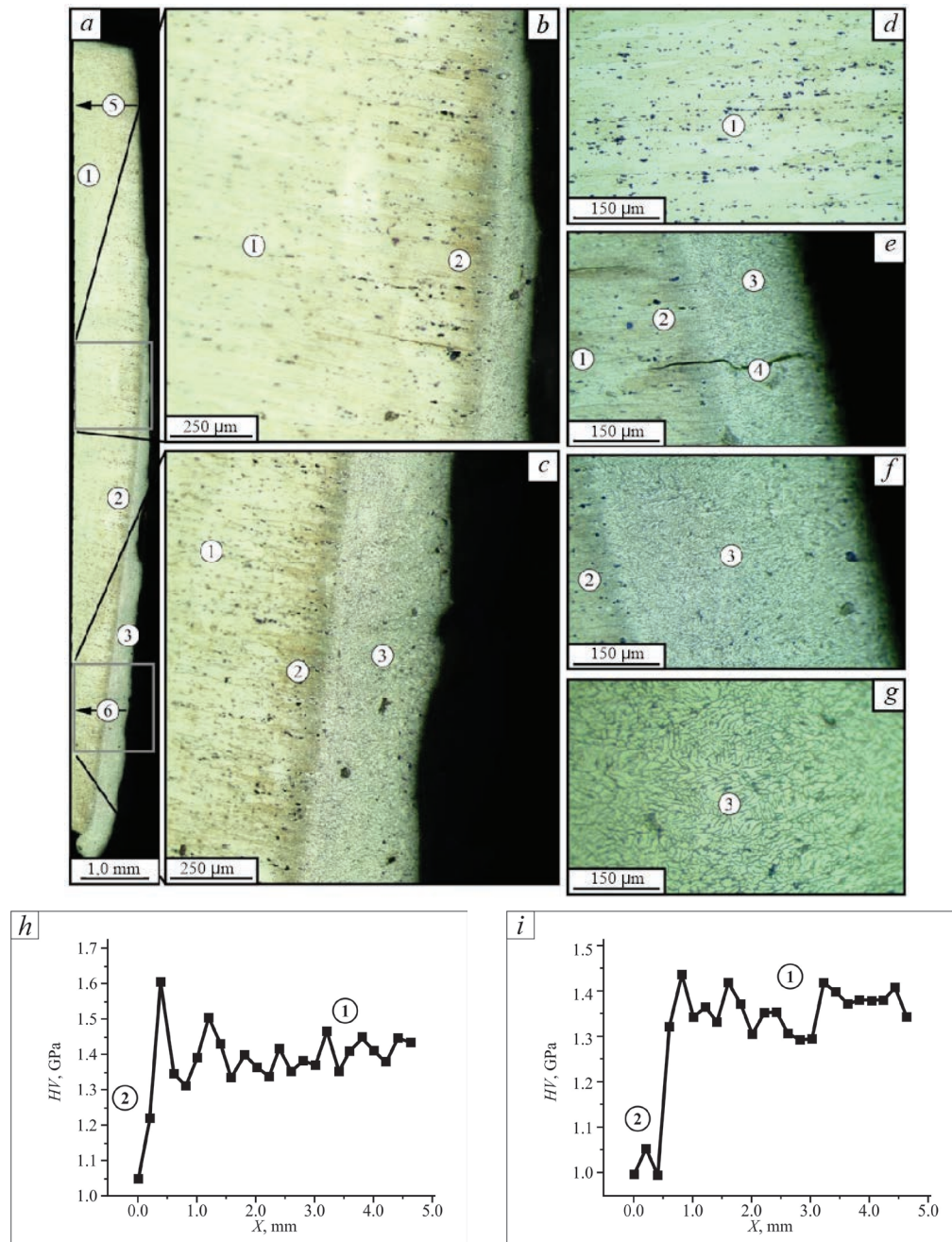


Fig. 8. Macro- and microstructure of typical specimen of aluminum alloy with a thickness of 12 mm after plasma cutting:

*a* – macrostructure; *b*, *c* – enlarged images of the upper and lower parts of cut zone; *d*–*g* – microstructure of specific zones; *h*, *i* – microhardness variation; 1 – base metal; 2 – heat-affected zone; 3 – melting zone; 4 – zone boundary; 5, 6 – areas of microhardness testing

The changes in mechanical properties in the cutting zone were observed on the specimens by measuring its microhardness (Fig. 8, *h*, *i*). The average value of the microhardness of the base metal of the specimens ranges from 1.35 to 1.45 GPa. In heat-affected zone and melting zone there is a sharp decrease of microhardness to the values 0.95–1.2 GPa which shows fairly significant decrease of mechanical properties in these zones. The boundary between the heat-affected zone and the base metal zone in the upper part of the sample is sharper than in the bottom part.

Macrostructure of AA2024 alloy specimens with a thickness of 40 mm obtained by different modes of plasma cutting is quite different from that described above (Fig. 9, *a*–*c*). The size of the heat-affected zone is significantly higher and amounts to 12–15 mm for most of the cutting modes. The smallest values of the

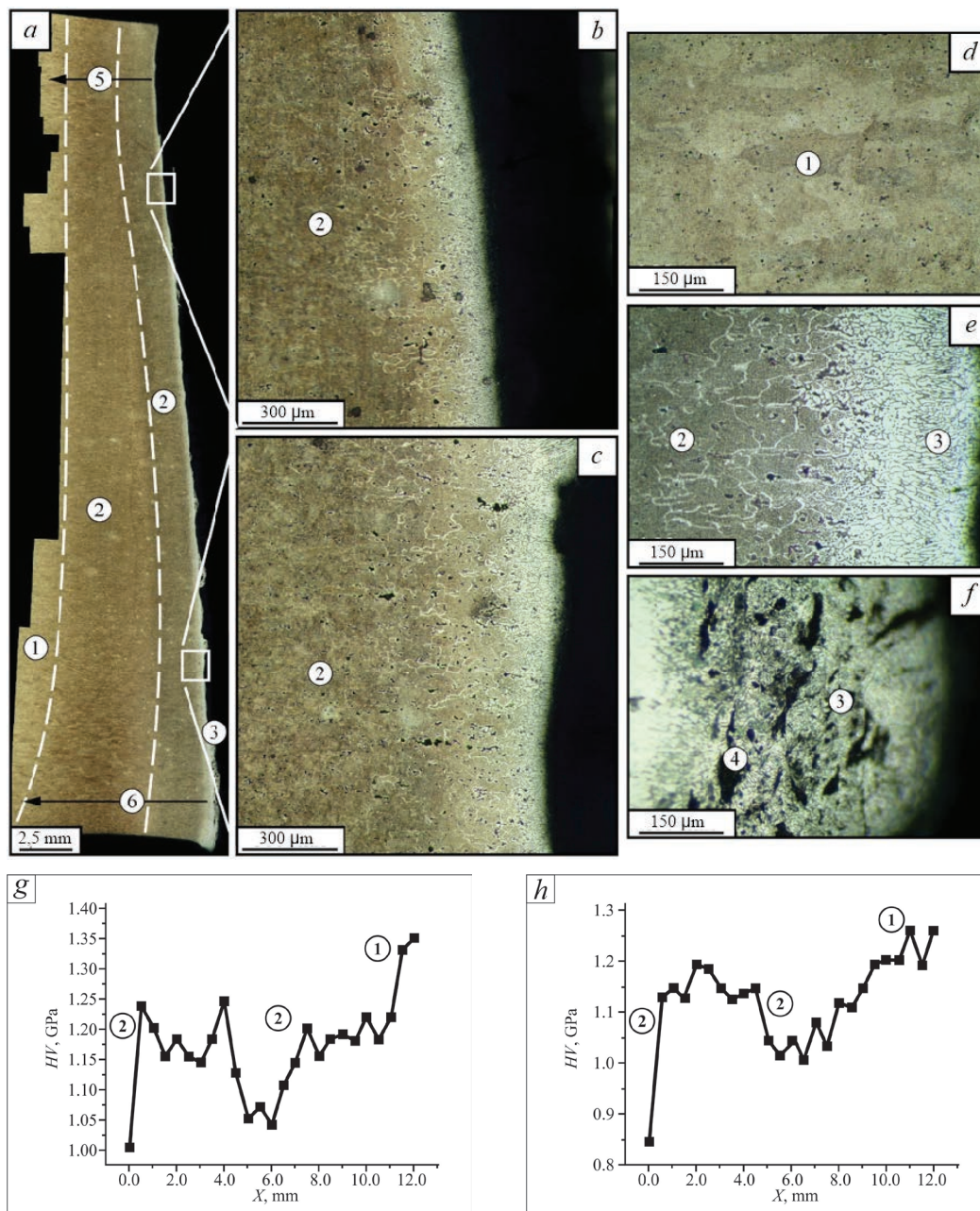


Fig. 9. Macro- and microstructure of typical specimen of aluminum alloy with a thickness of 40 mm after plasma cutting:

*a* – macrostructure; *b*, *c* – enlarged images of the upper and lower parts of cut zone; *d–f* – microstructure of specific zones; *g*, *h* – microhardness variation; 1 – base metal; 2 – heat-affected zone; 3 – melting zone; 4 – defects; 5, 6 – areas of microhardness testing

size of the heat-affected zone are characteristic for the mode No. 8, for which the size of the heat-affected zone is 4.0 mm in the upper part of the cut and 8.0 mm in the bottom part. For these specimens the deviation of cut geometry in the upper part, which is from 0.7 to 5.2 mm, is very important.

Studies of the structure of the specimens under higher magnification show that the structure of the material in different parts of the cutting zone is represented by structures quite similar to those identified for 12 mm thick specimens (Fig. 9, *d–e*). In the melting zone, the structure is represented by dendritic structure with a large number of pores and discontinuities. The heat-affected zone is characterized by increased etchability compared to the base metal; it can be further divided into two parts, also different in the degree of etching.

With the initial value of the microhardness of the material in 1.25–1.35 GPa, in the heat-affected zone, it is possible to reduce the microhardness to values of the order of 0.85–1.15 GPa (Fig. 9, *g*, *h*). According to changes in microhardness the heat-affected zone is also divided into two separate parts.

During cutting of *C1220* copper specimens with thickness of 40 mm it was found that, despite the large thickness of sheet, the size of heat-affected zone in the specimens is at a sufficiently low level (Fig. 10, *a-c*). The magnitude of deviation of macrogeometry of specimens cut is less than 0.7 mm. The size of the melting zone is up to 0.15 mm. The heat-affected zone is practically not visible on metallographic thin sections. Its grain structure is similar to that of the base metal (Fig. 10, *b-d*). There are a large number of pores, discontinuities and laminations in the melting zone (Fig. 10, *e,f*). The heat-affected zone was detected only when analyzing changes in the microhardness of the material in the cutting zone (Fig. 10, *g, h*). The size of the heat-affected zone is 0.5–3.0 mm, depending on the cutting mode. The smallest size is characteristic for the mode No. 7, which can be considered optimal from the viewpoint of the allowance for further machining.

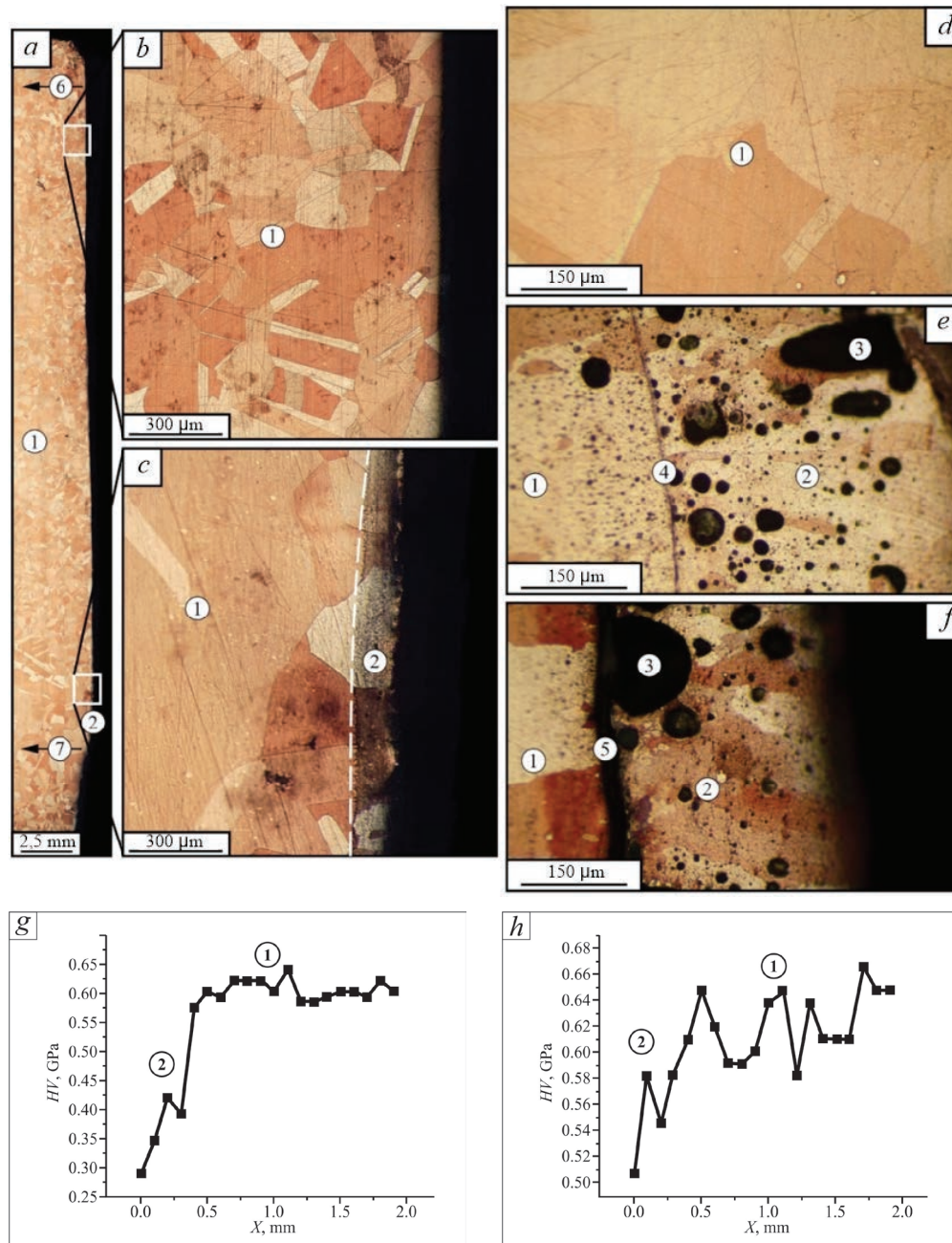


*Fig. 10.* Macro- and microstructure of typical specimen of copper with a thickness of 40 mm after plasma cutting:

*a*–macrostructure; *b, c*–enlarged images of the upper and lower parts of cut zone; *d–f*–microstructure of specific zones; *g, h*–microhardness variation; 1 – base metal; 2 – heat-affected zone; 3 – pores; 4, 5 – lamination; 6, 7 – areas of microhardness testing

## Conclusion

The research shows that for the cutting of *AA2024* aluminum alloy and *Ti-1.5Al-1.0Mn* titanium alloy with thickness up to 12 mm it is possible to regulate the cutting speed within a wide range, while for rolled *Cl220* copper and *AA2024* aluminum alloy with thickness of 40 mm the range of regulation of the cutting speed is quite narrow. Intensive heat removal of copper rolled products allows obtaining a cut with minimal values of a partial or complete melting zone, although it is possible to obtain rather large amounts of flowed metal in the cutting zone, consisting of melted metal pushed out of the cutting zone. Studies of the cutting processes of aluminum alloy *AA2024* and titanium alloy *Ti-1.5Al-1.0Mn* revealed the depth of thermal effect of cutting, changing from the top to the bottom of the cut. While for aluminum alloy *AA2024* due to excessive precipitation of alloying elements from a solid solution in a zone of thermal influence a decrease in microhardness was noted, for alloy titanium alloy *Ti-1.5Al-1.0Mn* microhardness growth caused by material hardening was characteristic.

The analysis of cut surface morphology, macro- and microstructure of the material in the cutting zone, as well as the study of microhardness changes allowed determining the most optimal combination of cutting mode parameters to obtain the most quality cuts. Changing the parameters of the cutting mode allows obtaining a more homogeneous macrogeometry of the cut surface, a smaller depth of the material remelting zone and the heat-affected zone, and smaller changes in the mechanical properties of the material in the cutting zone. For titanium alloy *Ti-1.5Al-1.0Mn* almost all used modes of cutting were close to optimum, though some of it provides a slightly better cut quality. (mode No. 2 when cutting specimens with thickness of 5 mm and mode No. 1 when cutting specimens with thickness of 10 mm). For aluminum alloy *AA2024* specimens with a thickness of 12 mm the best cutting mode was No. 2, and for the specimens with a thickness of 40 mm – mode No. 8. When cutting *Cl220* copper specimens with a thickness of 40 mm, the best quality of the cut was achieved with the mode No. 7. The obtained results are summarized in Table 2.

Table 2

Change in cut quality indicators depending on plasma cutting modes

Alloy	S, mm	Mode No.	Roughnesses, $\mu\text{m}$	Macrogeometry distortion, mm	Depth of the heat-affected zone, mm**
<i>Ti-1.5Al-1.0Mn</i>	5	1	75–275	0.5–0.6	0.5–1.8
<b><i>Ti-1.5Al-1.0Mn</i></b>	<b>5</b>	<b>2*</b>	<b>65–210</b>	<b>0.5–0.6</b>	<b>0.4–0.9</b>
<i>Ti-1.5Al-1.0Mn</i>	5	3	70–245	0.4–0.6	0.5–1.5
<b><i>Ti-1.5Al-1.0Mn</i></b>	<b>10</b>	<b>1*</b>	<b>150–330</b>	<b>0.6–1.9</b>	<b>0.3–0.4</b>
<i>Ti-1.5Al-1.0Mn</i>	10	2	110–450	0.6–2.3	0.3–0.4
<i>Ti-1.5Al-1.0Mn</i>	10	3	110–680	0.7–1.9	0.4–0.6
<i>AA2024</i>	12	1	50–80	1.3–1.5	0.5–0.8
<b><i>AA2024</i></b>	<b>12</b>	<b>2*</b>	<b>130–150</b>	<b>0.4–0.5</b>	<b>0.5–0.9</b>
<i>AA2024</i>	12	3	100–260	1.3–1.4	0.3–0.8
<i>AA2024</i>	12	4	50–80	2.0–2.3	0.4–0.9
<i>AA2024</i>	12	5	55–240	3.1–3.2	1.6–3.5
<i>AA2024</i>	40	1	210–510	0.9–1.0	12.6–15.6
<i>AA2024</i>	40	2	205–230	2.5–2.6	12.7–15.7
<i>AA2024</i>	40	3	350–460	2.7–2.9	1.7–15.7
<i>AA2024</i>	40	4	260–300	4.5–5.0	12.3–15.3
<i>AA2024</i>	40	5	200–470	0.6–0.7	12.5–12.75
<i>AA2024</i>	40	6	330–600	0.9–1.1	4.0–15.0
<i>AA2024</i>	40	7	320–550	5.0–5.2	5.0–15.0
<b><i>AA2024</i></b>	<b>40</b>	<b>8*</b>	<b>470–570</b>	<b>2.8–3.0</b>	<b>4.5–8.5</b>
<i>AA2024</i>	40	9	470–570	1.3–1.5	12.0–13.0
<i>AA2024</i>	40	10	125–520	1.1–1.3	13–16
<i>Cl220</i>	40	1	–	–	1.3–1.5

Change in cut quality indicators depending on plasma cutting modes

Alloy	S, mm	Mode No.	Roughnesses, $\mu\text{m}$	Macrogeometry distortion, mm	Depth of the heat-affected zone, mm**
CI220	40	2	–	–	0.8–0.9
CI220	40	3	–	–	0.65–0.75
CI220	40	4	80–180	1.2–1.4	2.8–3.0
CI220	40	5	25–75	0.5–0.7	1.9–2.0
CI220	40	6	7–65	1.0–1.2	2.7–3.0
<b>CI220</b>	<b>40</b>	<b>7*</b>	<b>45–200</b>	<b>0.9–1.0</b>	<b>1.8–1.9</b>

\* The most optimal plasma cutting modes

\*\* In this case, the depth of the thermal influence zone and the melting zone are included

Based on the results of the work, it can be concluded that plasma cutting at reverse polarity currents is effective for cutting rolled products of large thicknesses; however, the method requires further development in order to improve the quality of the resulting cut. In the future, it is planned to conduct comparative studies in the field of plasma cutting of rolled sheets of large thicknesses using plasma torches with forward and reverse polarity.

### References

1. Akkurt A. The effect of cutting process on surface microstructure and hardness of pure and Al 6061 aluminium alloy. *Engineering Science and Technology, an International Journal*, 2015, vol. 18, iss. 3, pp. 303–308. DOI: 10.1016/j.jestch.2014.07.004.
2. Ilii S.M., Coteata M. Plasma arc cutting cost. *International Journal of Material Forming*, 2009, vol. 2, pp. 689–692. DOI: 10.1007/s12289-009-0588-4.
3. Patel P., Nakum B., Abhishek K., Rakesh Kumar V., Kumar A. Optimization of surface roughness in plasma arc cutting of AISID2 steel using TLBO. *Materials Today: Proceedings*, 2018, vol. 5, iss. 9 (3), pp. 18927–18932. DOI: 10.1016/j.matpr.2018.06.242.
4. Bini R., Colosimo B.M., Kutlu A.E., Monno M. Experimental study of the features of the kerf generated by a 200A high tolerance plasma arc cutting system. *Journal of Materials Processing Technology*, 2008, vol. 196, iss. 1–3, pp. 345–355. DOI: 10.1016/j.jmatprotec.2007.05.061.
5. Hoult A.P., Pashby I.R., Chan K. Fine plasma cutting of advanced aerospace materials. *Journal of Materials Processing Technology*, 1995, vol. 48, iss. 1–4, pp. 825–831. DOI: 10.1016/0924-0136(94)01727-I.
6. Peko I., Nedic B., Djordjevic A., Dzunic D., Janković M., Veza I. Modeling of surface roughness in plasma jet cutting process of thick structural steel. *Tribology in Industry*, 2016, vol. 38, no. 4, pp. 522–529.
7. Andrés D., García T., Cicero S., Lacalle R., Álvarez J.A., Martín-Meizoso A., Aldazabal J., Bannister A., Klimpel A. Characterization of heat affected zones produced by thermal cutting processes by means of Small Punch tests. *Materials Characterization*, 2016, vol. 119, pp. 55–64. DOI: 10.1016/j.matchar.2016.07.017.
8. Gariboldi E., Previtali B. High tolerance plasma arc cutting of commercially pure titanium. *Journal of Materials Processing Technology*, 2005, vol. 160, iss. 1, pp. 77–89. DOI: 10.1016/j.jmatprotec.2004.04.366.
9. Nandan Sharma D., Ram Kumar J. Optimization of dross formation rate in plasma arc cutting process by response surface method. *Materials Today: Proceedings*, 2020, vol. 32, pt. 3, pp. 354–357. DOI: 10.1016/j.matpr.2020.01.605.
10. Gostimirović M., Rodic D., Sekulić M., Aleksic A. An experimental analysis of cutting quality in plasma arc machining. *Advanced Technologies and Materials*, 2020, vol. 45, no. 1, pp. 1–8. DOI: 10.24867/ATM-2020-1-001.
11. Kechagias J., Petousis M., Vidakis N., Mastorakis N. Plasma arc cutting dimensional accuracy optimization employing the parameter design approach. *ITM Web of Conferences*, 2017, vol. 9, p. 03004. DOI: 10.1051/itmconf/20170903004.
12. Cinar Z., Asmael M., Zeeshan Q. Developments in plasma arc cutting (PAC) of steel alloys: a review. *Jurnal Kejuruteraan*, 2018, vol. 30, pp. 7–16. DOI: 10.17576/jkukm-2018-30(1)-02.
13. Kudrna L., Fries J., Merta M. Influences on plasma cutting quality on CNC machine. *Multidisciplinary Aspects of Production Engineering*, 2019, vol. 2, pp. 108–117. DOI: 10.2478/mape-2019-0011.



14. Anakhov S., Guzanov B., Matushkin A., Pugacheva N., Pyckin Yu. Vliyanie konstruktivnykh osobennosti plazmotrona na kachestvo reza pri pretsizionnoivozdushno-plazmennoi razdelke metalla [Influence of plasma torch design on cutting quality during precision air-plasma cutting of metal]. *Izvestiya vysshikh uchebnykh zavedenii. Chernaya metallurgiya = Izvestiya. Ferrous Metallurgy*, 2020, vol. 63, no. 2, pp. 155–162. DOI: 10.17073/0368-0797-2020-2-155-162.

15. Peko I., Marić D., Nedić B., Samardžić I. Modeling and optimization of cut quality responses in plasma jet cutting of aluminium alloy EN AW-5083. *Materials*, 2021, vol. 14, iss. 19, p. 5559. DOI: 10.3390/ma14195559.

16. Salonitis K., Vatousianos S. Experimental investigation of the plasma arc cutting process. *Procedia CIRP*, 2012, vol. 3, pp. 287–292. DOI: 10.1016/j.procir.2012.07.050.

17. Suresh A., Diwakar G. Optimization of process parameters in plasma arc cutting for TWIP steel plates. *Materials Today: Proceedings*, 2021, vol. 38, pt. 5, pp. 2417–2424. DOI: 10.1016/j.matpr.2020.07.383.

18. Nemchinsky V. Erosion of thermionic cathodes in welding and plasma arc cutting systems. *IEEE Transactions on Plasma Science*, 2014, vol. 42, no. 1, pp. 199–215. DOI: 10.1109/TPS.2013.2287794.

19. Matushkina I., Anakhov S., Pyckin Yu. Design of a new gas-dynamic stabilization system for a metal-cutting plasma torch. *Journal of Physics: Conference Series*, 2021, vol. 2094, p. 042075. DOI: 10.1088/1742-6596/2094/4/042075.

20. Shchitsyn V.Yu., Yazovskikh V.M. Effect of polarity on the heat input into the nozzle of a plasma torch. *Welding International*, 2002, vol. 16 (6), pp. 485–487. DOI: 10.1080/09507110209549563.

21. Shicin Y.D., Belinin D.S., Kuchev P.S., Neulybin S.D. Osobennosti teploperedachi v izdelie pri rabote plazmotrona na toke obratnoi polyarnosti [Features of heat transfer to the product when working on the plasma torch current of reversed polarity]. *Vestnik Permskogo natsional'nogo issledovatel'skogo politekhnicheskogo universiteta. Mashinostroenie, materialovedenie = Bulletin PNRPU. Mechanical engineering, materials science*, 2014, vol. 16, no. 2, pp. 42–50. DOI: 10.15593/v16i2.3275.

22. Shitsyn Y.D., Shitsyn V.Y., Neulybin S.D., Nikulin R.G., Nikulina S.G., Karunakarah K.P. Issledovanie raboty anodov dugovykh plazmotronov dlya raboty na obratnoi polyarnosti toka [Investigation of the operation of the anodes of arc plasmatrons for operation on reverse polarity of current]. *Vestnik Permskogo natsional'nogo issledovatel'skogo politekhnicheskogo universiteta. Mashinostroenie, materialovedenie = Bulletin PNRPU. Mechanical engineering, materials science*, 2020, vol. 22, no. 3, pp. 60–67. DOI: 10.15593/2224-9877/2020.3.08.

## Conflicts of Interest

The authors declare no conflict of interest.

© 2022 The Authors. Published by Novosibirsk State Technical University. This is an open access article under the CC BY license (<http://creativecommons.org/licenses/by/4.0/>).

